Infectious Agents and Cancer

RESEARCH

Open Access

DNA hypomethylation modification promotes BST2 expression in cervical cancer by facilitating STAT1 binding to the promoter of BST2

Reziwanguli Wubuli[1], Zumurelaiti Ainiwaer[1], Mayinuer Niyazi[1] and Lili Han[1*]

Abstract

Cervical cancer (CC) is a common cancer that causes considerable morbidity and mortality, especially in developing countries. Bone marrow stromal cell antigen 2 (BST2) is a transmembrane glycoprotein, and its promoter methylation has been extensively documented in numerous human cancers. Nevertheless, the specific role of BST2 in CC remains unclear. This research utilized methylation-specific PCR (MSP), Western blotting, and RT-qPCR to evaluate the expression and DNA methylation levels of BST2 in CC tissues and cells. The role of STAT1 in regulating BST2 transcription was confirmed through dual-luciferase reporter assays and chromatin immunoprecipitation (ChIP) assays. Furthermore, we conducted experiments on cell proliferation, apoptosis, epithelial-mesenchymal transition (EMT), and xenograft tumor models to investigate the functional role and regulatory mechanisms of BST2 in CC, both in vitro and in vivo. We found that BST2 was increased in CC tissues and cells, promoting cell proliferation and EMT while inhibiting apoptosis. Mechanistically, BST2 upregulation was associated with hypomethylation of its promoter, potentially regulated by DNMT3a and DNMT3b. Furthermore, the transcription factor STAT1 was found to bind to the BST2 promoter, positively regulating its expression and thereby accelerating tumorigenesis in CC. Silencing BST2 significantly reduced tumor growth in vivo. Our findings highlight BST2 as a potential biomarker and therapeutic target in CC, with its expression regulated by DNA methylation and STAT1 binding.

Keywords Cervical cancer, BST2, Epigenetic regulation, DNA methylation, STAT1

*Correspondence:
Lili Han
18814115890@163.com
[1]Gynecological Medical Diagnosis and Treatment Center, People's Hospital of Xinjiang Uygur Autonomous Region, No.91, Tianchi Road, Tianshan District, Urumqi, Xinjiang 830001, China

Introduction

Cervical cancer (CC) ranks as one of the most prevalent malignant tumors among women worldwide, exhibiting significant morbidity and mortality rates, particularly in developing countries [1]. In China, both the incidence and mortality rates of CC are increasing each year, particularly in rural regions and areas with lower economic development [2]. Persistent infection with high-risk human papillomavirus (HPV), particularly types HPV16 and HPV18, is the primary factor contributing to the development of CC [3]. A range of genetic mutations, such as PIK3CA [4], along with various epigenetic modifications [5], including DNA methylation and histone modifications [6], are found in CC cells. These changes significantly contribute to tumorigenesis, disease progression, and the overall phenotype of the condition. Currently, the primary strategies for preventing CC include organized cytology-based screening programs, HPV screening, and HPV vaccination [7]. CC is a highly preventable malignancy that can be effectively managed when identified in its early stages [8]. Surgery is the main treatment for early-stage CC, resulting in high survival rates [9]. Radiotherapy, chemotherapy, and immunotherapy are used for advanced or recurrent cases, with notable efficacy yet significant side effects and costs [10]. Therefore, investigating the pathogenesis of CC, identifying new biomarkers, therapeutic targets, and novel therapies are crucial for enhancing the survival rates and quality of life for CC patients.

Bone marrow stromal cell antigen 2 (BST2), commonly referred to as Tetherin or CD317, encodes a type II transmembrane glycoprotein that plays a significant role in various biological processes, especially in antiviral defense and tumor development [11]. BST2 exhibits abnormal expression in multiple tumors and is strongly linked to tumor advancement and patient outcomes. For example, Kuang et al. indicated that the downregulation of BST2 sensitized nasopharyngeal carcinoma cells to cisplatin and promoted apoptosis by inhibiting the activation of the NF-κB pathway [12]. Xu et al. illustrated that BST2 expression was elevated in hepatocellular carcinoma, correlating with larger tumor size, increased tumor multiplicity, and poorer overall survival [13]. Notably, Liu et al. showed that BST2 expression was markedly increased in CC cells, and silencing BST2 suppressed cell proliferation, migration, invasion, and M2 macrophage polarization, while promoting apoptosis [14]. In summary, the expression of BST2 was notably increased in CC; however, the molecular mechanisms by which its pro-carcinogenic effects are mediated require further investigation.

DNA methylation, as an epigenetic modification, involves the addition of methyl groups to the 5' carbon position of cytosine within a DNA molecule, resulting in the formation of 5-methylcytosine (5-mC) through the action of DNA methyltransferases (DNMTs) [15]. This process primarily occurs in the CpG islands located in the promoter regions of genes [16]. While it does not change the DNA sequence itself, it can influence gene expression by altering chromatin structure and affecting the interaction of transcription factors [17–19]. In pathological conditions, abnormal patterns of DNA methylation may result in either gene silencing or activation, which can disrupt normal cellular functions [20]. Furthermore, aberrant DNA methylation has been investigated in CC, and is regarded as a significant mechanism contributing to the development and progression of the disease [21]. For example, Bo et al. uncovered that oncogenic lncRNA AFAP1-AS1 was increased and hypomethylated in CC, and depletion of AFAP1-AS1 repressed migration, invasion, and epithelial-mesenchymal transition (EMT) process [22]. Su et al. suggested that ZEB1 expression was regulated by TET1-mediated DNA methylation modifications and histone interactions, and TET1 promoted stemness and inhibited EMT by increasing 5hmC and altering histone methylation at the ZEB1 promoter, thereby suppressing ZEB1 expression and potentially blocking CC development [23]. DNA methylation modification by BST2 has not yet been documented in CC; however, its involvement in other types of cancer has been investigated. For instance, the increased expression of BST2 was associated with its hypomethylation in breast cancer [24]. In our study, we aimed to investigate whether BST2 expression in CC is regulated by DNA methylation modifications.

Signal transducer and activator of transcription 1 (STAT1) is a member of the STAT protein family of transcription factors, and plays an important role in cell signaling and the regulation of gene expression [25, 26]. In tumors, STAT1 serves a dual function. On one hand, the activation of STAT1 demonstrates tumor suppressor functions in certain tumors by facilitating apoptosis and suppressing proliferation [27]. Conversely, in other tumors, STAT1 may be inappropriately activated, which can enhance tumor cell survival and facilitate immune evasion [28, 29]. In particular, Wu et al. indicated that STAT1 was increased in CC, and a positive correlation between STAT1 expression and HPV16 viral load in carcinogenesis of CC [30]. Besides, recent studies have demonstrated a significant interaction between STAT1 and BST2. STAT1 can bind to the promoter region of the BST2 gene, directly affecting its transcriptional activity. For example, in oral squamous cell carcinoma cells, STAT1 was essential for regulating the BST2 promoter region, specifically, STAT1 influenced the transcription of BST2, leading to an elevated expression of BST2 [31]. Verma et al. demonstrated that STAT1 suppressed the invasion of HTR-8/SVneo cells by enhancing the

expression of BST2 in the presence of IFN-γ treatment [32]. Taken together, we hypothesized that STAT1 may play an important role in the tumorigenesis of CC by regulating the expression of BST2 and affecting the biological behavior of CC cells.

The purpose of this research was to explore how DNA hypomethylation enhances BST2 expression through the binding of STAT1 to the BST2 promoter. This study may provide a theoretical basis and potential targets for the diagnosis and treatment of CC.

Materials and methods

Patients and samples

In our research, CC tissues and matched adjacent noncancerous tissues were collected from twenty patients at the People's Hospital of the Xinjiang Uygur Autonomous Region. The study received approval from the Ethics Committee of the People's Hospital of the Xinjiang Uygur Autonomous Region, and written informed consent was obtained from all participants. None of the patients had received chemotherapy or radiotherapy before their surgical resection. Following excision, tissues were immediately snap-frozen in liquid nitrogen and stored at − 80 °C for subsequent analysis.

Cell culture and treatment

HeLa, SiHa, and normal cervical epithelial cells (HcerEpic) were obtained from Shanghai Yaji Biotechnology Co., Ltd. The cells were maintained in high-glucose DMEM (Gibco, Carlsbad, USA) supplemented with 10% heat-inactivated fetal bovine serum (FBS) (Gibco, Carlsbad, USA) and cultured at 37 °C in a humidified incubator with 5% CO_2 and 95% air. For the experiments, HeLa and SiHa cells were seeded at a density of 1×10^5 cells per well in a 6-well plate. In addition, cells were treated with 5 μM 5-aza-CdR (Sigma-Aldrich, St. Louis, USA) for 72 h, after which they were collected for further analysis.

Vectors and transfection

HeLa and SiHa cells were seeded at a density of 1×10^5 cells per well in 6-well plates. Cells were transfected with either a negative control (NC) or siRNAs targeting BST2, DNMT1, DNMT3a, DNMT3b, and STAT1 using the siRNA Transmate reagent (Suzhou GenePharma Co., Ltd.). Transfection was performed at 37 °C for 6 h, after which the medium was replaced with fresh medium. For overexpression experiments, HeLa and SiHa cells were transfected with either the BST2 overexpression plasmid (oe-BST2; pcDNA3.1 vector, NM_004335.4, 1.5 μg/well) or a negative control plasmid (oe-NC; empty pcDNA3.1 vector, 1.5 μg/well) using Lipofectamine™ 3000 reagent (Invitrogen; Thermo Fisher Scientific, Inc.) at 37 °C. Cells were harvested for further experiments 24 h post-transfection. The siRNA sequences and the plasmids were obtained from Suzhou GenePharma Co., Ltd.

Lentiviral vectors targeting BST2 were produced using a second-generation system in 293T cells. Cells were transfected with GV vector (20 μg), pHelper 1.0 (15 μg), and pHelper 2.0 (10 μg) using Lipofectamine 3000. After 6 h, the medium was replaced, and supernatants were collected 48 h later, centrifuged, and concentrated by ultracentrifugation. The viral titer was 1×10^8 TU/ml. SiHa cells were transduced at a multiplicity of infection (MOI) of 50 in the presence of polybrene (8 μg/ml), followed by puromycin selection (2 μg/ml). Finally, viral titers and knockdown efficiency were validated.

RNA extraction and RT-qPCR

Total RNA was extracted from cells or tissues using the UNIQ-10 column Trizol total RNA extraction kit (Sangon Biotech). Complementary DNA (cDNA) was synthesized from 1 μg of total RNA using PrimeScript RT Master Mix (Takara Bio) according to the manufacturer's instructions. The reverse transcription reaction was performed at 37 °C for 15 min, followed by inactivation at 85 °C for 5 s and cooling to 4 °C using a PCR Veriti thermal cycler (Applied Biosystems).

Quantitative PCR (qPCR) was performed using the QuantStudio®5 Real-Time PCR System (Applied Biosystems) with iTaq Universal SYBR Green Supermix (Bio-Rad Laboratories). The thermal cycling conditions included an initial denaturation at 95 °C for 3 min, followed by 40 cycles of 95 °C for 15 s and 60 °C for 1 min. Primer sequences are listed in Table 1. Relative gene expression was normalized to GAPDH and calculated using the $2^{-\Delta\Delta Ct}$ method.

Table 1 Sequences of primers for RT-qPCR

Name	Forward (5′-3′)	Reverse (5′-3′)
BST2	CACACTGTGATGGCCCTAATG	GTCCGCGATTCTCACGCTT
E-cadherin	ATTGCTCACATTTCCCAACTC	GTCACCTTCAGCCATCCT
Snail	GGCTCCTTCGTCCTTCTCCTCTAC	CCAGGCTGAGGTATTCCTTGTTGC
Vimentin	GAGAACTTTGCCGTTGAAGC	TCCAGCAGCTTCCTGTAGGTG
DNMT1	CGGCTTCAGCACCTCATTTG	AGGTCGAGTCGGAATTGCTC
DNMT3a	GCCTGAAGCCTCAAGAGCAGT	TTTAGCCACGACCCAGACCAT
DNMT3b	CCCAGCTCTTACCTTACCATCG	GGTCCCCTATTCCAAACTCCT
STAT1	CAGCTTGACTCAAAATTCCTGGA	TGAAGATTACGCTTGCTTTTCCT

Western blot analysis

Tissues or cells were lysed in RIPA buffer containing PMSF (100:1) at 4 °C for 30 min. Subsequently, the lysate was subjected to centrifugation at 10,000×g for 10 min at 4 °C to obtain the supernatants. The protein concentration was determined using a BCA protein assay kit (Beijing Solarbio Science & Technology Co., Ltd.). A total of 20 μg of protein per lane was separated by SDS-PAGE and transferred to PVDF membranes (Invitrogen; Thermo Fisher Scientific, Inc.). Membranes were blocked with 5% non-fat milk for 2 h at room temperature and incubated overnight at 4 °C with primary antibodies, including anti-BST2 (1:1,000; cat. no. ab243230; Abcam), anti-DNMT1 (1:1,000; cat. no. sc-514784; Santa Cruz Biotechnology), anti-DNMT3a (1:1,000; cat. no. 3598; Cell Signaling Technology), anti-DNMT3b (1:1,000; cat. no. sc-393845; Santa Cruz Biotechnology), anti-STAT1 (1:1,000; cat. no. ab234400; Abcam), anti-cleaved Caspase-3 (1:1000, cat. no. 9661; Cell Signaling Technology), anti-γH2AX (1:1000, cat. no. 2577; Cell Signaling Technology), and anti-GAPDH (1:1,000; cat. no. sc-137179; Santa Cruz Biotechnology). Following washing with TBST, the membranes were incubated with HRP-conjugated secondary antibodies (1:10,000; Bioworld Technology, Inc.) for 1 h at 25 °C. Protein bands were visualized using the Amersham Imager 680 (Cytiva) along with ECL reagent (MilliporeSigma), and the quantification of protein expression was performed using ImageJ software (version 1.46; National Institutes of Health), with GAPDH serving as the loading control.

Cell proliferation assay

Cell proliferation was assessed using the Cell Counting Kit-8 (CCK-8; Beyotime Institute of Biotechnology). After transfection, cells were seeded into 96-well plates at a density of 5×10^3 cells per well and cultured at 37 °C in a humidified incubator with 5% CO_2. At 0, 24, 48, 72, and 96 h post-seeding, 10 μl of CCK-8 solution was added to each well. The plates were incubated for 2 h at 37 °C, and the absorbance was measured at 450 nm using a microplate reader (Thermo Fisher Scientific, Inc.).

Cell apoptosis assay

Cell apoptosis was evaluated 48 h post-transfection utilizing the Annexin V-FITC/PI Apoptosis Detection Kit (Beyotime Biotechnology, Shanghai, China). Briefly, treated cells were collected and washed twice with cold phosphate-buffered saline (PBS). The resulting cell pellet was then resuspended in 1× Binding Buffer at a concentration of 1×10^6 cells/ml. A volume of 100 μl of this cell suspension was placed into a flow cytometry tube and stained with 5 μl of Annexin V-FITC and 10 μl of propidium iodide (PI) for a duration of 15 min at room temperature in the absence of light. After staining, 400 μl of 1× Binding Buffer was added to the cells. Apoptosis was subsequently assessed using a flow cytometer (BD FACSCalibur), and the data were processed with FlowJo software (Tree Star, Inc.). Early apoptotic cells were characterized as Annexin V-FITC-positive and PI-negative, whereas late apoptotic and necrotic cells were identified as Annexin V-FITC-positive and PI-positive.

Animal studies

Female BALB/c nude mice (6 to 8 weeks old) were utilized for the xenograft experiment. SiHa cells, which had undergone stable BST2 knockdown (kd-BST2) or this controls (kd-NC), were collected and subcutaneously injected into the right flank (3×10^6 cells/100 μl). After a period of 28 days, the mice were euthanized, and the tumors were removed for subsequent analysis. Tumor volume was determined using the formula: volume = (length × width^2)/2.

DNA methylation analysis

Genomic DNA was isolated from HeLa and SiHa cell lines and subsequently quantified utilizing a NanoDrop spectrophotometer (Thermo Fisher Scientific, USA). The bisulfite conversion of the genomic DNA was conducted using the EpiTect Bisulfite Kit (Qiagen, Germany), following the guidelines provided by the manufacturer. For methylation-specific PCR (MSP), the converted DNA was amplified with primers specifically designed to target the region of interest. The resulting PCR products were subjected to separation on a 2% agarose gel (Invitrogen, USA) and visualized through staining with GelRed (Biotium, USA) under ultraviolet light. The methylation status was assessed by analyzing the presence or absence of distinct bands that corresponded to either methylated or unmethylated alleles.

Dual-luciferase reporter assay

The promoter region of BST2 was amplified via PCR with specific primers and subsequently cloned into the pGL3-Basic luciferase reporter vector (Promega, USA). Bioinformatics analysis was employed to identify the STAT1-binding sites within the BST2 promoter, and mutations were introduced utilizing the QuikChange Site-Directed Mutagenesis Kit (Agilent, USA). The sequences of both the wild-type (WT) and mutant (MUT) promoters were verified through Sanger sequencing. Cells were plated at a density of 1×10^4 cells per well in 96-well plates. Co-transfection of cells was performed with 100 ng of either BST2-WT or BST2-MUT promoter constructs alongside 10 ng of the pRL-TK Renilla luciferase vector (Promega, USA), using Lipofectamine 3000 reagent (Invitrogen, USA). The total amount of DNA was adjusted with an empty pGL3-Basic vector to maintain consistent transfection efficiency. After a 48-h

incubation, cells were lysed, and luciferase activity was assessed using the Dual-Luciferase Reporter Assay System (Promega, USA). Firefly luciferase activity was normalized against Renilla luciferase activity to correct for variations in transfection efficiency and cell viability.

Chromatin Immunoprecipitation (ChIP)

Chromatin immunoprecipitation (ChIP) assays were conducted on HeLa and SiHa cell lines, as well as on clinical and nude mouse tissues, utilizing the Magna ChIP™ G Kit (MilliporeSigma, USA) in accordance with the manufacturer's guidelines. In summary, the samples were subjected to crosslinking with 1% formaldehyde for 10 min at room temperature to ensure the stabilization of protein-DNA interactions, followed by a quenching step with 0.125 M glycine. Subsequently, the samples were lysed and sonicated with a Bioruptor® Plus sonication device (Diagenode, Belgium) to fragment the chromatin into pieces measuring approximately 200–500 bp. The resulting lysates were centrifuged, and the supernatants were retained for immunoprecipitation, which was carried out overnight at 4 °C using either an anti-STAT1 antibody (Cell Signaling Technology, USA) or IgG as a negative control. Immune complexes were isolated using protein G magnetic beads, followed by washing and elution. The crosslinks were then reversed, and DNA was purified through a spin column. The enrichment of the BST2 promoter region was assessed via quantitative PCR (qPCR) employing specific primers designed for the BST2 promoter.

Statistical analysis

Data obtained from three separate experiments were evaluated utilizing GraphPad Prism 9 and SPSS 19.0. The results are presented as mean ± standard deviation (SD). For statistical comparisons, either Student's t-test or one-way ANOVA with Tukey's test was employed, with non-parametric tests applied when necessary. A p-value of less than 0.05 was considered statistically significant.

Results

BST2 is highly expressed in cervical cancer tissues and cell lines

Initially, we investigated the expression of BST2 in CC tissues and cells. As shown in Fig. 1A, the mRNA expression levels of BST2 were greatly higher in CC tumor

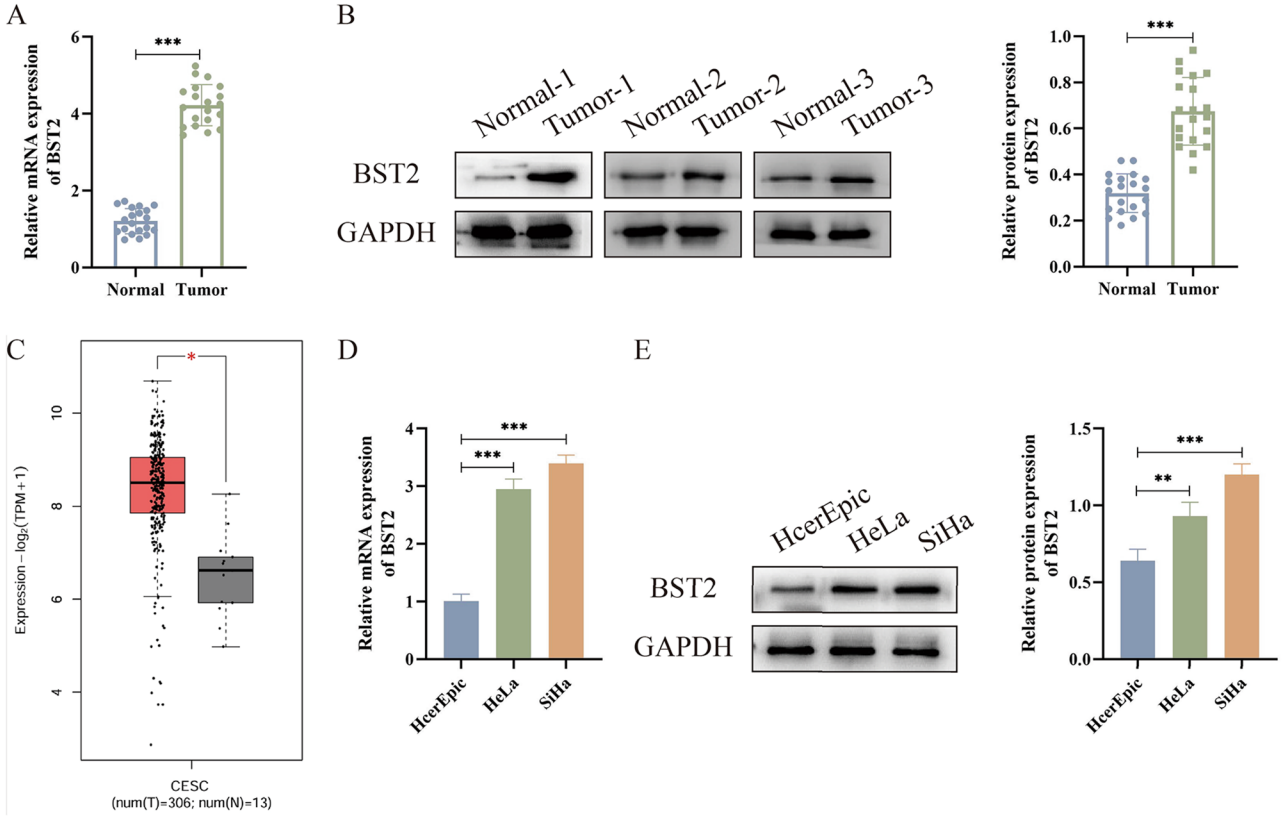

Fig. 1 BST2 is highly expressed in cervical cancer tissues and cell lines. (**A**) The mRNA expression levels of BST2 in cervical cancer tumor tissues compared to normal tissues, as determined by RT-qPCR. (**B**) Protein expression levels of BST2 in tumor tissues and normal tissues were analyzed by Western blot. (**C**) Expression levels of BST2 in cervical squamous cell carcinoma (CESC) tissues and normal tissues were assessed using the GEPIA2 database. (**D**-**E**) The mRNA and protein levels of BST2 in HcerEpic, HeLa, and SiHa cells were measured by RT-qPCR and Western blot, respectively. *$p < 0.05$, **$p < 0.01$, ***$p < 0.001$

tissues compared to adjacent normal tissues. Western blot analysis revealed that CC tumor tissues exhibited elevated protein expression levels of BST2 in comparison to normal tissues (Fig. 1B). Moreover, an analysis conducted using the GEPIA2 database showed that BST2 expression levels were notably elevated in cervical squamous cell carcinoma (CESC) tissues when compared to normal tissues (Fig. 1C). Besides, RT-qPCR analysis indicated that BST2 mRNA expression levels were increased in HeLa and SiHa cells compared to HcerEpic cells (Fig. 1D). Similarly, Western blot analysis demonstrated that HeLa and SiHa cells exhibited a significantly higher BST2 expression compared to HcerEpic cells (Fig. 1E). These data showed that the increased BST2 expression was observed in CC tissues and cell lines, indicating its potential as a biomarker or therapeutic target in CC.

Silencing BST2 alleviates tumorigenesis of cervical cancer in vitro and in vivo

To explore the biological function of BST2 in CC, we transfected BST2 knockdown vectors in HeLa and SiHa cells. The knockdown efficiency of BST2 in both cell lines was successfully validated by both RT-qPCR (Fig. 2A) and Western blot analysis (Fig. 2B). There was a significant reduction in the relative mRNA and protein expression levels of BST2 in both BST2-silenced HeLa and SiHa cells (Fig. 2A-B). Cell viability assays conducted with the CCK-8 method indicated that silencing BST2 decreased the viability of HeLa and SiHa cells (Fig. 2C-D). Flow cytometry analysis revealed that the proportion of apoptotic cells was notably higher in BST2-depleted HeLa and SiHa cells than in the control cells (Fig. 2E), indicating that silencing BST2 induced apoptosis in both HeLa and SiHa cells. Additionally, we found that the expression of cleaved caspase-3 and γH2AX was increased in BST2-depleted HeLa and SiHa cells (Fig. 2F). RT-qPCR analysis of EMT-related genes suggested that the expression of E-cadherin was increased, whereas the levels of Snail and Vimentin were suppressed in both HeLa and SiHa cells upon BST2 knockdown (Fig. 2G). Moreover, to explore the effect of BST2 on tumor growth, we constructed a xenograft model by injecting SiHa cells that were stably transfected with either the BST2 knockdown vector or a negative control vector into nude mice. Our results showed that the BST2 expression was effectively suppressed in kd-BST2 group of nude mice (Fig. 2H). The tumor size was notably smaller in the BST2 knockdown group compared to the control group (Fig. 2I). Besides, both tumor weight and volume were markedly lower in BST2-depleted group compared to control group (Fig. 2J), suggesting that silencing BST2 effectively blocked tumor growth in vivo. This data collectively demonstrated that silencing BST2 effectively inhibited CC development both in vitro and in vivo, indicating that BST2 may serve as a potential therapeutic target for CC treatment.

Upregulation of BST2 in cervical cancer cells is associated with hypomethylation of the BST2 promoter

To explore the epigenetic regulation of BST2 in CC, we first assessed the methylation status of its promoter. Bioinformatic analysis revealed the presence of a CpG island within the BST2 promoter region, indicating a potential site for DNA methylation regulation (Fig. 3A). Methylation-specific PCR (MSP) demonstrated that BST2 exhibited hypomethylation in HeLa and SiHa cells when compared to normal cervical epithelial cells (HcerEpic) (Fig. 3B). The application of the DNA methyltransferase inhibitor 5-aza-CdR notably increased BST2 expression in both HeLa and SiHa cells, as assessed by RT-qPCR (Fig. 3C). Knockdown experiments further elucidated the role of DNMTs in regulating BST2 expression. As shown in Fig. 3D, silencing DNMT1 led to a notable elevation in BST2 mRNA expression in SiHa cells, whereas no such increase was observed in HeLa cells. In addition, Western blot analysis uncovered that there were no significant changes in BST2 protein levels in either HeLa or SiHa cells (Fig. 3E-G). Furthermore, inhibition of DNMT3a led to increased BST2 mRNA and protein expression in both HeLa and SiHa cells (Fig. 3H-J). Similarly, suppression of DNMT3b also led to upregulation of BST2 mRNA and protein expression in both CC cell lines (Fig. 3K-M). The findings suggested that DNMT3a and DNMT3b, but not DNMT1, may play crucial roles in regulating BST2 expression through DNA methylation. Taken together, our results demonstrated that hypomethylation of the BST2 promoter contributed to its upregulation in CC cells.

The transcription factor STAT1 contributes to the expression of BST2

Transcription factors are essential in the regulation of genes and the advancement of diseases. To explore the regulatory function of the transcription factor STAT1 in CC, we examined its interaction with BST2. Inhibition of STAT1 in HeLa and SiHa cells led to a notable reduction in the expression levels of STAT1 and BST2 mRNA as well as their corresponding proteins (Fig. 4A-B), suggesting that STAT1 may positively regulate BST2 transcription. Conversely, silencing BST2 did not lead to any notable changes in the expression of STAT1 mRNA and protein (Fig. 4C-D). This suggested that the regulatory relationship was unidirectional, whereby STAT1 influenced BST2, but the reverse was not true. Dual-luciferase reporter assays validated the interaction between STAT1 and the BST2 promoter, as evidenced by a notable decrease in luciferase activity when STAT1-specific mutations were introduced in the BST2 promoter region

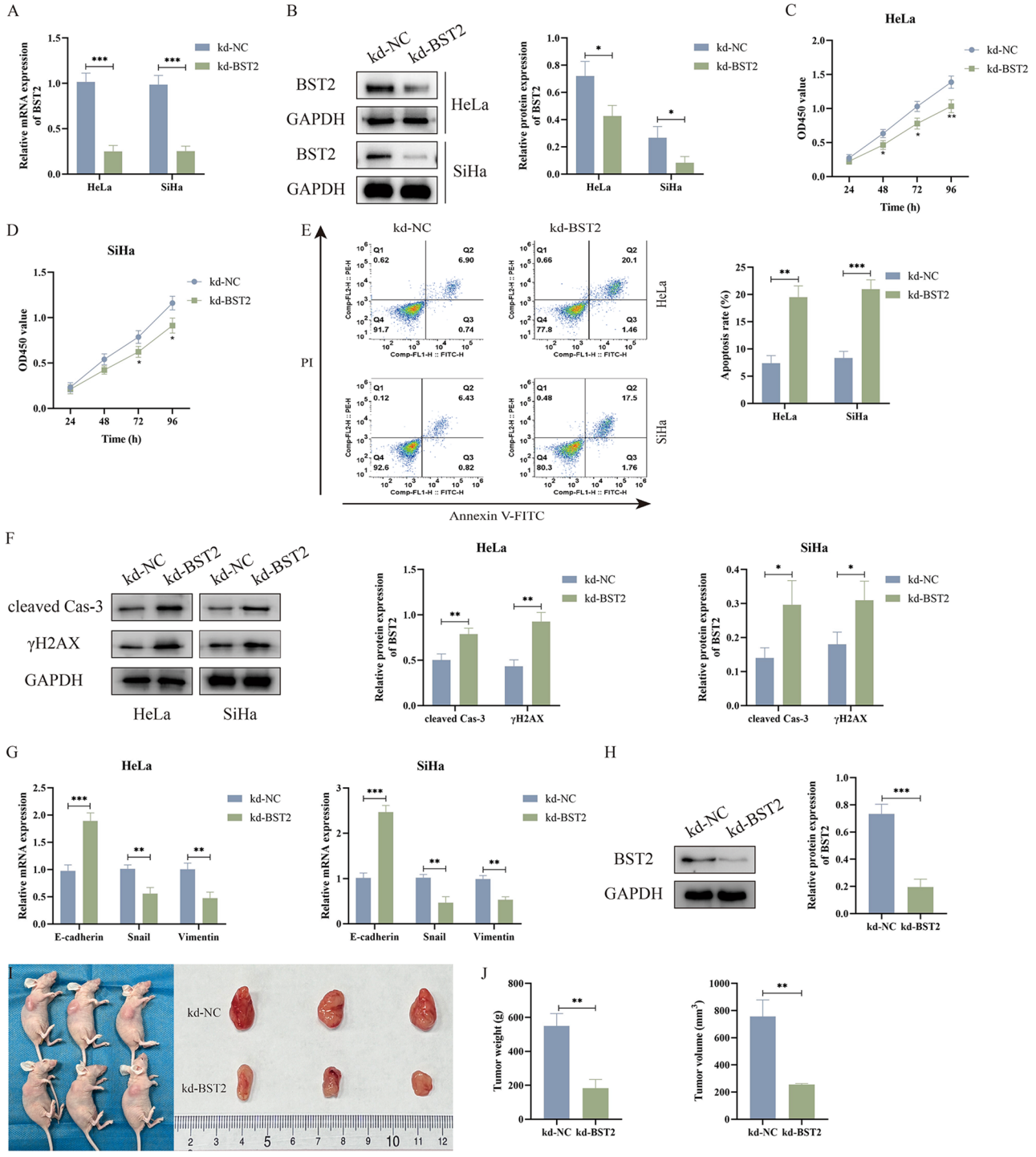

Fig. 2 Silencing BST2 alleviates tumorigenesis of cervical cancer in vitro and in vivo. (**A**-**B**) Knockdown efficiency of BST2 in HeLa and SiHa cells, as detected by RT-qPCR and Western blot. (**C**-**D**) Cell viability assay (CCK-8) in control and BST2-depleted HeLa and SiHa cells. (**E**) Analysis of cell apoptosis using flow cytometry. (**F**) The levels of cleaved caspase-3 and γH2AX were detected by Western blot. (**G**) RT-qPCR analysis of epithelial-mesenchymal transition (EMT) related genes E-cadherin, Snail, and Vimentin. (**H**) The expression of BST2 protein in xenograft tumors was assessed by Western blot. (**I**) Representative images of xenograft tumors injected with SiHa cells. (**J**) Tumor weight and volume measurements of xenograft tumors. $^{*}p < 0.05$, $^{**}p < 0.01$, $^{***}p < 0.001$

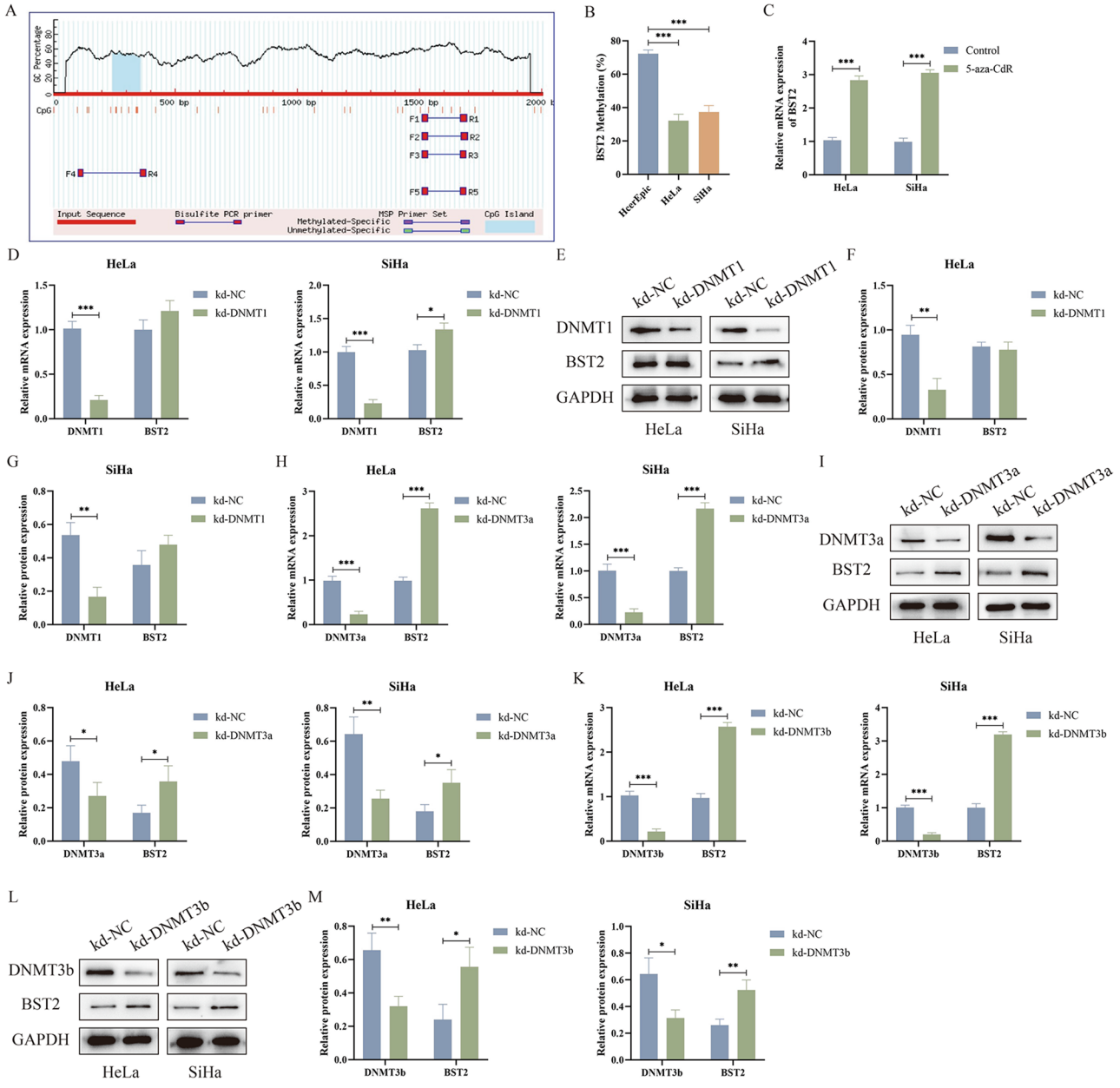

Fig. 3 Upregulation of BST2 in cervical cancer cells is associated with hypomethylation of the BST2 promoter. (**A**) CpG island location within the BST2 gene promoter region. (**B**) Methylation levels of BST2 in HcerEpic, HeLa, and SiHa cells were examined by MSP. (**C**) BST2 expression levels in control and 5-aza-CdR treated HeLa and SiHa cells were measured by RT-qPCR. (**D**-**G**) RT-qPCR and Western blot assessed the mRNA and protein levels of DNMT1 and BST2 in DNMT1-silenced HeLa and SiHa cells. (**H**-**J**) The mRNA and protein levels of DNMT3a and BST2 in DNMT3a-depleted HeLa and SiHa cells were detected by RT-qPCR and Western blot. (**K**-**M**) The mRNA and protein levels of DNMT3b and BST2 in HeLa and SiHa cells after knockdown DNMT3b were measured by RT-qPCR and Western blot. *$p < 0.05$, **$p < 0.01$, ***$p < 0.001$

(Fig. 4E). To further validate this interaction, a ChIP assay was performed. The results showed that STAT1 increased the expression levels of BST2 through promoting its transcription in both cell lines and CC tumor tissues, however, in a nude mouse xenograft model, the ability of the BST2 promoter to enrich STAT1 was significantly reduced in the kd-STAT1 group compared to the control group (Fig. 4F). Additionally, we also detected the expression levels of STAT1 in CC. STAT1 mRNA and protein levels were elevated in tumor tissues compared to the normal paraneoplastic tissues (Fig. 4G-H). Among the cell lines tested, STAT1 mRNA and protein expression were elevated in HeLa and SiHa cells (Fig. 4I-J). Besides, a positive correlation between STAT1 and BST2 expression in CESC was identified (Fig. 4K), which further substantiates the involvement of STAT1 in the regulation of BST2 expression. These researches uncovered that STAT1 positively regulated BST2 expression in CC.

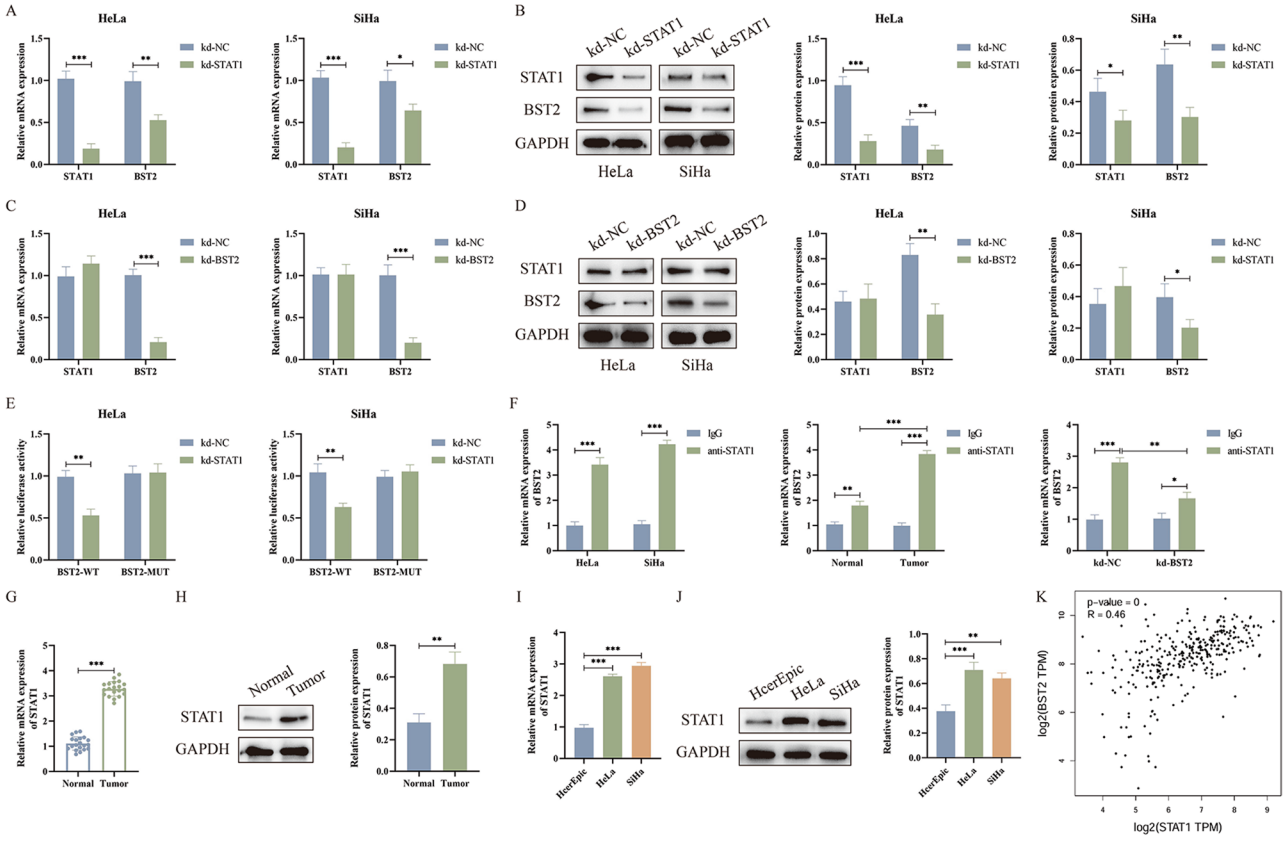

Fig. 4 The transcription factor STAT1 contributes to the expression of BST2. (**A**-**B**) The mRNA and protein expression of STAT1 and BST2 in STAT1-silenced cervical cancer cells. (**C**-**D**) The mRNA and protein expression of STAT1 and BST2 in BST2-silenced cervical cancer cells. (**E**) Dual-luciferase reporter assay verifying the binding site of STAT1 to the BST2 promoter. (**F**) The binding ability of STAT1 to the BST2 promoter in cervical cancer cells, clinical tissues and xenograft tumor was detected using a chromatin immunoprecipitation assay. (**G**-**H**) The mRNA and protein expression of STAT1 in normal and cervical cancer tissues. (**I**-**J**) The mRNA and protein expression of STAT1 in HcerEpic, HeLa, and SiHa cells. (**K**) A high correlation between STAT1 and BST2 in CESC was shown by GEPIA dataset analysis. *$p < 0.05$, **$p < 0.01$, ***$p < 0.001$

STAT1 positively regulates BST2 expression to exacerbate cervical cancer progression

To investigate whether STAT1 contributes to CC progression through regulation of BST2, we knockdown STAT1 while overexpressing BST2 to detect its effect on cellular functions. First, the transfection efficiency of overexpressed BST2 in both HeLa and SiHa cells was examined by RT-qPCR and Western blot analysis (Fig. 5A-B). The CCK-8 assay uncovered that silencing STAT1 hampered cell proliferation in both HeLa and SiHa cells, conversely, the overexpression of BST2 in STAT1-depleted CC cells partially reversed this proliferation impairment (Fig. 5C-D). Flow cytometry analysis illustrated that inhibition of STAT1 induced cell apoptosis in both HeLa and SiHa cells, whereas the overexpression of BST2 effectively rescued this pro-apoptotic effect (Fig. 5E-F). Simultaneously, RT-qPCR analysis revealed that the upregulation of E-cadherin and the decrease of Snail and Vimentin were observed in STAT1-silenced HeLa and SiHa cells, indicating that depletion of STAT1 repressed the EMT process (Fig. 5G). However, the inhibitory effect on EMT induced by knockdown STAT1 was restored by co-treatment with a BST2 overexpression vector (Fig. 5G). In summary, these findings showed that STAT1 positively regulated BST2 expression, which in turn promoted cell proliferation, EMT process and suppressed cell apoptosis.

Discussion

CC is a prevalent cancer affecting the female reproductive system [33]. In recent years, significant advancements have been made in the prevention and treatment of CC through the extensive use of diverse methods; however, the outcomes for late-stage treatment remain inadequate [34]. Therefore, it is necessary to elucidate the molecular mechanisms that induce the progression of CC. The expression of BST2 is abnormally elevated in various malignant tumors, including gastric cancer [35], colorectal cancer [36], ovarian cancer [37], and CC [14]. Consistent with previous research, we demonstrated that BST2 was overexpressed in CC tissues and cell lines when compared with adjacent normal tissues and normal cervical epithelial cells (HcerEpic). Additionally, depletion of

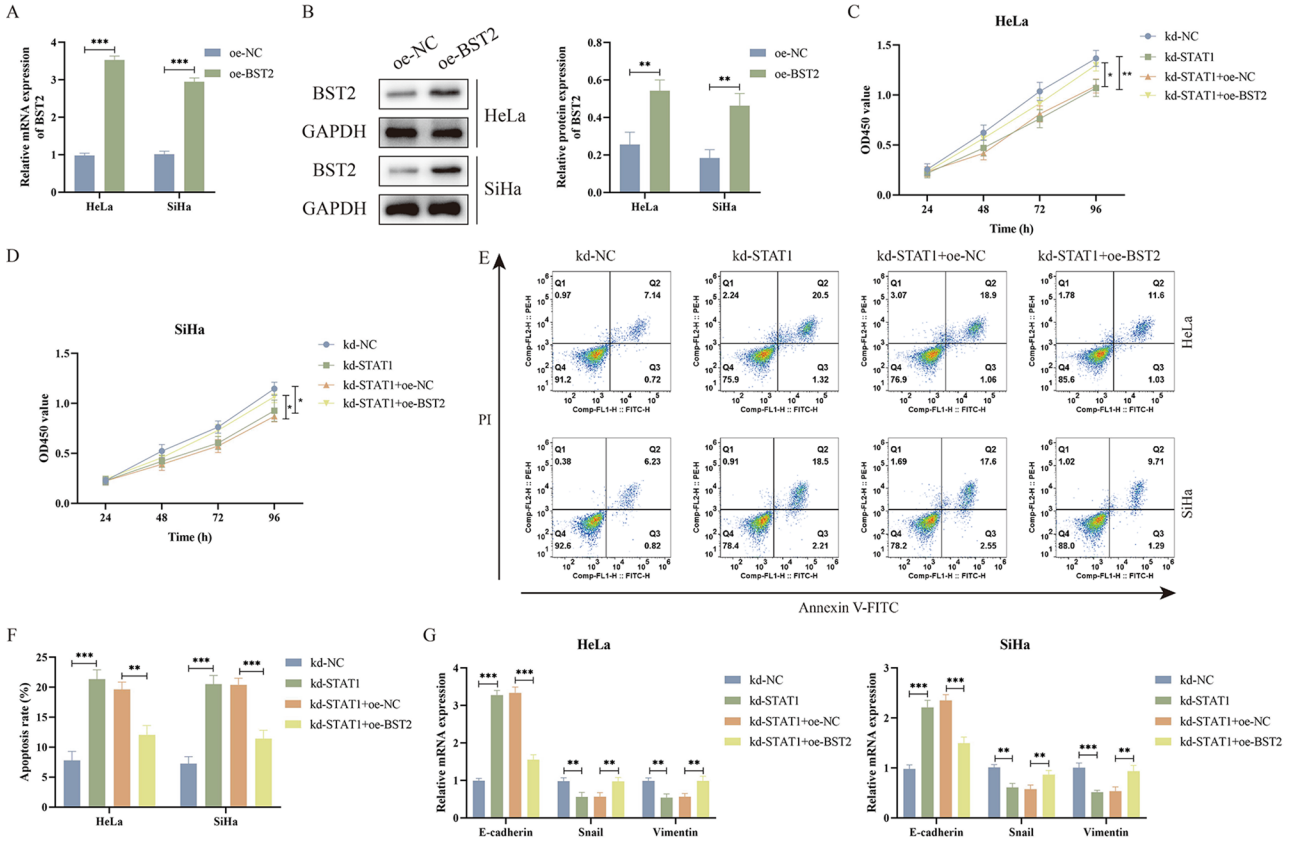

Fig. 5 STAT1 positively regulates BST2 expression to exacerbate cervical cancer progression. (**A**-**B**) BST2 expression in HeLa and SiHa cells transfected with a BST2 overexpressing vector was measured by RT-qPCR and Western blot. (**C**-**D**) Cell viability was measured by CCK-8 assay in kd-NC, kd-STAT1, kd-STAT1 + oe-NC, and kd-STAT1 + oe-BST2 groups of HeLa and SiHa cells. (**E**-**F**) Analysis of cell apoptosis using flow cytometry. (**G**) RT-qPCR assessment of E-cadherin, Snail, and Vimentin levels. *$p < 0.05$, **$p < 0.01$, ***$p < 0.001$

BST2 through siRNA interference resulted in decreased cell proliferation, increased apoptosis, and repressed EMT in HeLa and SiHa cells. Besides, the knockdown of BST2 also blocked the tumor growth in vivo. As a novel biomarker and a promising therapeutic target, BST2 is expected to provide innovative insights into the diagnosis, prognostic evaluation, and treatment approaches for CC.

DNA methylation is crucial in the development and advancement of multiple diseases, as it regulates gene expression, preserves genome stability, and affects cellular functions [38]. Reports have indicated that the promoter region of the BST2 gene contains a CpG island, and its methylation status is crucial for regulating gene expression [24]. For instance, the research conducted by Singh et al. explored the relationship between the expression levels of BST2 and the impact of DNA methylation on the regulation of HIV-1 viral load in black women. The findings revealed that higher levels of BST2 were associated with better viral control, suggesting that BST2 could serve as a promising therapeutic target for HIV and related conditions [39]. Furthermore, DNMTs influence gene expression by modifying the methylation of promoter regions. Xi et al. indicated that DNMT1 facilitated the methylation of miR-20a, thereby suppressing its expression in retinal pigment epithelium cells affected by of diabetic retinopathy [40]. Xu et al. uncovered that DNMT3b down-regulated miR-34a expression through increasing miR-34a promoter methylation in bladder cancer [41]. In our study, we found that the upregulation of BST2 was associated with the DNA hypomethylation of the BST2 promoter. Additionally, in CC cells, the demethylation of BST2 may be facilitated by DNMT3a and/or DNMT3b, but not by DNMT1. Nonetheless, the involvement of DNMTs in the progression of CC through the regulation of BST2 requires further investigation.

Transcription factors regulate gene transcription by binding to promoter or enhancer regions, thereby affecting cellular biological functions and potentially playing a role in disease progression [42]. As a crucial transcription factor, STAT1 exerts significant influence in cancer development, yet its role as either an oncogene or a tumor suppressor is highly context-dependent, depending on the particular genetic context [43]. For instance, Zhang et al. uncovered that STAT1 interacted with the CircIFI30 promoter to increase its transcriptional

activity, thus aggravating malignant progression of triple-negative breast cancer [25]. Ai et al. suggested that the transcription factor STAT1 can enhance a malignant cell phenotype through the upregulation of LINC01160 in nasopharyngeal carcinoma [44]. Strikingly, STAT1 has been identified as a crucial transcription factor responsible for the increased expression of BST2 in both oral squamous cell carcinoma and complications associated with pregnancy [31, 32]. Our data indicated that STAT1 positively regulated the expression of BST2 in CC cells. Functional experiments demonstrated that silencing STAT1 inhibited cell proliferation and EMT, and promoted cell apoptosis. Conversely, overexpression of BST2 effectively reversed the inhibitory effects observed in STAT1-depleted CC cells. Taken together, these data illustrated that STAT1 increased BST2 level through the regulation of its promoter region.

In conclusion, the present study uncovered the role of BST2 in CC, demonstrating that BST2 expression was upregulated through DNA methylation and STAT1 binding to its promoter, contributing to tumor progression by promoting cell survival, inhibiting apoptosis, and facilitating EMT. In addition, our research has certain limitations. Firstly, the limited sample size may impact the statistical validity and generalizability of the findings. Secondly, while BST2 has demonstrated potential as a biomarker and therapeutic target in CC, its specific application in clinical diagnosis and treatment requires additional validation. In summary, this research explored the cancer-promoting function of STAT1 in CC, along with the impact of BST2 promoter hypomethylation and the regulatory role of STAT1 in its expression. This offers a significant theoretical foundation for identifying new therapeutic targets for CC and creating personalized treatment strategies.

Supplementary Information

The online version contains supplementary material available at https://doi.org/10.1186/s13027-025-00670-2.

Supplementary Material 1

Author contributions

Reziwanguli Wubuli conceived and designed the study. Zumurelaiti Ainiwaer performed the experiments and analyzed the data. Mayinuer Niyazi wrote the manuscript and conducted experimental verification. Lili Han supervised and revised the manuscript.

Funding

Our study was supported by the Natural Science Foundation of Xinjiang Uygur Autonomous Region Project (2022D01C105).

Data availability

The data are available upon a reasonable request to the corresponding author.

Declarations

Ethics approval and consent to participate

This research was approved by the Ethics Committee of the People's Hospital of Xinjiang Uygur Autonomous Region. All animal experiments were conducted in accordance with the guidelines established by the Committee and complied with the internationally recognized ARRIVE guidelines.

Competing interests

The authors declare no competing interests.

Received: 18 March 2025 / Accepted: 22 May 2025
Published online: 13 June 2025

References

1. Wang L, Zhao Y, Wang Y, Wu X. The Role of Galectins in Cervical Cancer Biology and Progression. Biomed Res Int. 2018:2175927. https://doi.org/10.1155/2018/2175927
2. Yuan M, Zhao X, Wang H, Hu S, Zhao F. Trend in cervical Cancer incidence and mortality rates in China, 2006–2030: A bayesian Age-Period-Cohort modeling study. Cancer Epidemiol Biomarkers Prev. 2023;32(6):825–33. https://doi.org/10.1158/1055-9965.Epi-22-0674.
3. Wei F, Georges D, Man I, Baussano I, Clifford GM. Causal attribution of human papillomavirus genotypes to invasive cervical cancer worldwide: a systematic analysis of the global literature. Lancet. 2024;404(10451):435–44. https://doi.org/10.1016/s0140-6736(24)01097-3.
4. Krishnamurthy S, Yoda H, Hiraoka K, Inoue T, Lin J, Shinozaki Y, et al. Targeting the mutant PIK3CA gene by DNA-alkylating pyrrole-imidazole polyamide in cervical cancer. Cancer Sci. 2021;112(3):1141–9. https://doi.org/10.1111/cas.14785.
5. Fang J, Zhang H, Jin S. Epigenetics and cervical cancer: from pathogenesis to therapy. Tumour Biol. 2014;35(6):5083–93. https://doi.org/10.1007/s13277-014-1737-z.
6. Liu H, Ma H, Li Y, Zhao H. Advances in epigenetic modifications and cervical cancer research. Biochim Biophys Acta Rev Cancer. 2023;1878(3):188894. https://doi.org/10.1016/j.bbcan.2023.188894.
7. Viveros-Carreño D, Fernandes A, Pareja R. Updates on cervical cancer prevention. Int J Gynecol Cancer. 2023;33(3):394–402. https://doi.org/10.1136/ijgc-2022-003703.
8. Pimple SA, Mishra GA. Global strategies for cervical cancer prevention and screening. Minerva Ginecol. 2019;71(4):313–20. https://doi.org/10.23736/s0026-4784.19.04397-1.
9. Poddar P, Maheshwari A. Surgery for cervical cancer: consensus & controversies. Indian J Med Res. 2021;154(2):284–92. https://doi.org/10.4103/ijmr.IJMR_4240_20.
10. Francoeur AA, Monk BJ, Tewari KS. Treatment advances across the cervical cancer spectrum. Nat Rev Clin Oncol. 2025;22(3):182–99. https://doi.org/10.1038/s41571-024-00977-w.
11. Yu H, Bian Q, Wang X, Wang X, Lai L, Wu Z, et al. Bone marrow stromal cell antigen 2: tumor biology, signaling pathway and therapeutic targeting (Review). Oncol Rep. 2024;51(3). https://doi.org/10.3892/or.2024.8704.
12. Kuang CM, Fu X, Hua YJ, Shuai WD, Ye ZH, Li Y, et al. BST2 confers cisplatin resistance via NF-κB signaling in nasopharyngeal cancer. Cell Death Dis. 2017;8(6):e2874. https://doi.org/10.1038/cddis.2017.271.
13. Xu X, Wang Y, Xue F, Guan E, Tian F, Xu J, et al. BST2 promotes tumor growth via multiple pathways in hepatocellular carcinoma. Cancer Invest. 2020;38(5):329–37. https://doi.org/10.1080/07357907.2020.1769125.
14. Liu G, Du X, Xiao L, Zeng Q, Liu Q. Activation of FGD5-AS1 promotes progression of cervical Cancer through regulating BST2 to inhibit macrophage M1 polarization. J Immunol Res. 2021;2021:p5857214. https://doi.org/10.1155/2021/5857214.
15. Koch A, Joosten SC, Feng Z, de Ruijter TC, Draht MX, Melotte V, et al. Analysis of DNA methylation in cancer: location revisited. Nat Rev Clin Oncol. 2018;15(7):459–66. https://doi.org/10.1038/s41571-018-0004-4.
16. Yamashita K, Hosoda K, Nishizawa N, Katoh H, Watanabe M. Epigenetic biomarkers of promoter DNA methylation in the new era of cancer treatment. Cancer Sci. 2018;109(12):3695–706. https://doi.org/10.1111/cas.13812.
17. Davie JR, Sattarifard H, Sudhakar SRN, Roberts CT, Beacon TH, Muker I, et al. Basic Epigenetic Mech Subcell Biochem. 2025;108:1–49. https://doi.org/10.1007/978-3-031-75980-2_1.

18. Li S, Peng Y, Panchenko AR, DNA methylation. Precise modulation of chromatin structure and dynamics. Curr Opin Struct Biol. 2022;75:102430. https://doi.org/10.1016/j.sbi.2022.102430.
19. Kribelbauer JF, Lu XJ, Rohs R, Mann RS, Bussemaker HJ. Toward a mechanistic Understanding of DNA methylation readout by transcription factors. J Mol Biol. 2020;432(6):1801–15. https://doi.org/10.1016/j.jmb.2019.10.021.
20. Nishiyama A, Nakanishi M. Navigating the DNA methylation landscape of cancer. Trends Genet. 2021;37(11):1012–27. https://doi.org/10.1016/j.tig.2021.05.002.
21. Zhu H, Zhu H, Tian M, Wang D, He J, Xu T. DNA methylation and hydroxymethylation in cervical cancer: diagnosis, prognosis and treatment. Front Genet. 2020;11:347. https://doi.org/10.3389/fgene.2020.00347.
22. Bo H, Fan L, Gong Z, Liu Z, Shi L, Guo C, et al. Upregulation and hypomethylation of LncRNA AFAP1–AS1 predicts a poor prognosis and promotes the migration and invasion of cervical cancer. Oncol Rep. 2019;41(4):2431–9. https://doi.org/10.3892/or.2019.7027.
23. Su PH, Hsu YW, Huang RL, Chen LY, Chao TK, Liao CC, et al. TET1 promotes 5hmC-dependent stemness, and inhibits a 5hmC-independent epithelial-mesenchymal transition, in cervical precancerous lesions. Cancer Lett. 2019;450:53–62. https://doi.org/10.1016/j.canlet.2019.01.033.
24. Mahauad-Fernandez WD, Borcherding NC, Zhang W, Okeoma CM. Bone marrow stromal antigen 2 (BST-2) DNA is demethylated in breast tumors and breast cancer cells. PLoS ONE. 2015;10(4):e0123931. https://doi.org/10.1371/journal.pone.0123931.
25. Zhang J, Xia S, Liu X, Qi D, He X, Chen D. STAT1 mediates the transcription of CircIFI30 and promotes the progression of Triple-Negative breast Cancer by Up-Regulating CDCA4. J Environ Pathol Toxicol Oncol. 2022;41(1):1–13. https://doi.org/10.1615/JEnvironPatholToxicolOncol.2021039794.
26. Kostanian IA, Vonarshenko AV, Lipkin VM. [STAT1: a many-sided transcription factor]. Bioorg Khim. 2010;36(1):15–28.
27. Wong GL, Manore SG, Doheny DL, Lo HW. STAT family of transcription factors in breast cancer: pathogenesis and therapeutic opportunities and challenges. Semin Cancer Biol. 2022;86(3):84–106. https://doi.org/10.1016/j.semcancer.2022.08.003.
28. Zhang L, Li Q, Yang J, Xu P, Xuan Z, Xu J, et al. Cytosolic TGM2 promotes malignant progression in gastric cancer by suppressing the TRIM21-mediated ubiquitination/degradation of STAT1 in a GTP binding-dependent modality. Cancer Commun (Lond). 2023;43(1):123–49. https://doi.org/10.1002/cac2.12386.
29. Dong G, Wang Q, Wen M, Xia Z, Zhang S, Gao W, et al. DDX18 drives tumor immune escape through transcription-activated STAT1 expression in pancreatic cancer. Oncogene. 2023;42(40):3000–14. https://doi.org/10.1038/s41388-023-02817-0.
30. Wu S, Wu Y, Lu Y, Yue Y, Cui C, Yu M, et al. STAT1 expression and HPV16 viral load predict cervical lesion progression. Oncol Lett. 2020;20(4):28. https://doi.org/10.3892/ol.2020.11889.
31. Shan F, Shen S, Wang X, Chen G. BST2 regulated by the transcription factor STAT1 can promote metastasis, invasion and proliferation of oral squamous cell carcinoma via the AKT/ERK1/2 signaling pathway. Int J Oncol. 2023;62(4). https://doi.org/10.3892/ijo.2023.5502.
32. Verma S, Kang AK, Pal R, Gupta SK. BST2 regulates interferon gamma-dependent decrease in invasion of HTR-8/SVneo cells via STAT1 and AKT signaling pathways and expression of E-cadherin. Cell Adh Migr. 2020;14(1):24–41. https://doi.org/10.1080/19336918.2019.1710024.
33. Yadav M, Kumar HS, Kumar R, Sharma N, Jakhar SL. Survival pattern in cervical cancer patients in North West India: A tertiary care center study. J Cancer Res Ther. 2022;18(6):1530–6. https://doi.org/10.4103/jcrt.jcrt_342_21.
34. Li H, Yuan Y, Dong H, Wang T, Zhang D, Zhou L, et al. Foxo3a-Mediated DNMT3B impedes cervical Cancer cell proliferation and migration capacities through suppressing PTEN promoter methylation. J Invest Surg. 2023;36(1):2162170. https://doi.org/10.1080/08941939.2022.2162170.
35. Liu W, Cao Y, Guan Y, Zheng C. BST2 promotes cell proliferation, migration and induces NF-κB activation in gastric cancer. Biotechnol Lett. 2018;40(7):1015–27. https://doi.org/10.1007/s10529-018-2562-z.
36. He X, Chen H, Zhong X, Wang Y, Hu Z, Huang H, et al. BST2 induced macrophage M2 polarization to promote the progression of colorectal cancer. Int J Biol Sci. 2023;19(1):331–45. https://doi.org/10.7150/ijbs.72538.
37. Yang LQ, Hu HY, Han Y, Tang ZY, Gao J, Zhou QY, et al. CpG-binding protein CFP1 promotes ovarian cancer cell proliferation by regulating BST2 transcription. Cancer Gene Ther. 2022;29(12):1895–907. https://doi.org/10.1038/s41417-022-00503-z.
38. Kulis M, Esteller M. DNA methylation and cancer. Adv Genet. 2010;70:27–56. https://doi.org/10.1016/b978-0-12-380866-0.60002-2.
39. Singh R, Ramsuran V, Naranbhai V, Yende-Zuma N, Garrett N, Mlisana K, et al. Epigenetic regulation of BST-2 expression levels and the effect on HIV-1 pathogenesis. Front Immunol. 2021;12:669241. https://doi.org/10.3389/fimmu.2021.669241.
40. Xi X, Wang M, Chen Q, Ma J, Zhang J, Li Y. DNMT1 regulates miR-20a/TXNIP-mediated pyroptosis of retinal pigment epithelial cells through DNA methylation. Mol Cell Endocrinol. 2023;577:112012. https://doi.org/10.1016/j.mce.2023.112012.
41. Xu K, Chen B, Li B, Li C, Zhang Y, Jiang N, et al. DNMT3B Silencing suppresses migration and invasion by epigenetically promoting miR-34a in bladder cancer. Aging. 2020;12(23):23668–83. https://doi.org/10.18632/aging.103820.
42. Bushweller JH. Targeting transcription factors in cancer - from undruggable to reality. Nat Rev Cancer. 2019;19(11):611–24. https://doi.org/10.1038/s41568-019-0196-7.
43. Zhang Y, Liu Z. STAT1 in cancer: friend or foe? Discov Med. 2017;24(130):19–29.
44. Ai J, Tan G, Wang T, Li W, Gao R, Song Y, et al. Transcription factor STAT1 promotes the proliferation, migration and invasion of nasopharyngeal carcinoma cells by upregulating LINC01160. Future Oncol. 2021;17(1):57–69. https://doi.org/10.2217/fon-2020-0618.

Publisher's note